Journal of the Korean Astronomical Society
54: 183 ∼ 190, 2021 December

https://doi.org/10.5303/JKAS.2021.54.6.183
pISSN: 1225-4614 · eISSN: 2288-890X
http://jkas.kas.org

One-Dimensional Treatment of Molecular Line Radiative Transfer in Clumpy Clouds

Yong-Sun Park
Department of Physics and Astronomy, Seoul National University, Gwanak-gu, Seoul 08826, Korea; yongsunp@snu.ac.kr

Received September 29, 2021; accepted November 22, 2021

Abstract: We have revisited Monte Carlo radiative transfer calculations for clumpy molecular clouds. Instead of introducing a three-dimensional geometry to implement clumpy structure, we have made use of its stochastic properties in a one-dimensional geometry. Taking into account the reduction of spontaneous emission and optical depth due to clumpiness, we have derived the excitation conditions of clumpy clouds and compared them with those of three-dimensional calculations. We found that the proposed approach reproduces the excitation conditions in a way compatible to those from three-dimensional models, and reveals the dependencies of the excitation conditions on the size of clumps. When bulk motions are involved, the applicability of the approach is rather vague, but the one-dimensional approach can be an excellent proxy for more rigorous three-dimensional calculations.

Key words: line: formation — radiative transfer — methods: numerical — ISM: molecules — ISM: clouds

1. Introduction

In order to analyze the properties of molecular clouds, one needs radiative transfer (RT) models of molecular transitions, which link the physical conditions of molecular clouds and and observables, namely the line profiles of multiple transitions. Therefore, radiative transfer models have been developed since the detection of molecules, including CO. In general, molecular clouds are turbulent and have complicated structures on all scales due to dynamical energy and momentum inputs from the environment and their large Reynolds numbers. Moreover, since molecular clouds typically have low densities, the non-LTE approach in three-dimensional geometry is crucial.

Non-LTE modelling initially used simple geometries. Goldreich & Kwan (1974) developed the large velocity gradient (LVG) model, importing the escape probability method applied to expanding stellar envelopes and ignored radiative interactions between locations separated from each other in a cloud because of the large velocity gradient. A modern version without systematic motion was developed by van der Tak et al. (2007).

The full non-LTE modeling for one-dimensional geometries of spheres or finite slabs began just after the LVG model by Leung & Liszt (1976). However, non-LTE radiative transfer models using Monte Carlo methods developed by Bernes (1979) are now commonly used, and many variations have been devised (Juvela & Padoan 2005). In these models, small numbers of model photons replacing copious real photons are generated and are allowed to travel through the medium. Then the number of (de-)excitations is counted for each zone and fed into the statistical equilibrium equations. Random numbers are generated and used to assign positions of photon production, frequency offset with respect to its rest frequency, and propagation directions. A major advantage of the model is that it can treat velocity fields accurately. Increasingly efficient methods have been developed since then to accelerate iterations and to reduce noise inherent in the Monte Carlo algorithm (Hogerheijde & van der Tak 2000).

Extension to three-dimensional space was accomplished later in the '90s based on the Monte Carlo methods (Park & Hong 1995; Juvela 1998; Brinch & Hogerheijde 2010). These three-dimensional radiative transfer models are often combined with three-dimensional (magneto-)hydrodynamic calculations (Quenard et al. 2017).

Three dimensional RT models are complex and require a large amount of computer resources. Here we propose an efficient one-dimensional RT model for clouds with complicated structures. As a simple approximation, a molecular cloud can be regarded as an aggregation of small clumps; in this case, the locations of individual clumps are not important. The clumpy cloud is a kind of stochastic system, and the distribution of clumps can be described by a statistical parameter: the volume filling factor. Then one may efficiently solve the RT problem for the clumpy molecular cloud in one dimension using the mean value without working in three-dimensional space.

Section 2 develops a one-dimensional approach to the stochastic systems and describes modifications to the existing one-dimensional Monte Carlo code. In Section 3, we present the results of one-dimensional calculations for the various combinations of input parameters and compare them with those from three-dimensional calculations. A summary and conclusions are given in

Corresponding author: Y.-S. Park

Section 4.

2. ONE-DIMENSIONAL RADIATIVE TRANSFER MODELS IN CLUMPY CLOUDS

2.1. Cloud Geometry

We assume a spherical molecular cloud composed of many small clumps. Such a clumpy structure has been suggested by observations (Moore & Marscher 1995; Molaro et al. 2016; Rybarczyk et al. 2020). The interclump medium may be taken into account, but for simplicity, we assume in this work that the space between clumps is empty. Observations suggest a high density contrast between clumps and interclump medium (Blitz & Stark 1986; Hennebelle & Falgarone 2012). Even a low density may play a role for CO, but we defer this to later studies. Clump density, temperature, and volume filling factor may have dependencies on the radial distance from the cloud center, but again for simplicity, we assume uniform values for these. The volume filling factor f is defined as the ratio of the volume occupied by clumps and the total volume. Cloud model parameters are adopted as follows: a kinetic temperature of $T_{\rm k} = 15$ K, a cloud radius of $R = 1$ pc, clump densities of $n(H_2) = 1 \times 10^3, 2 \times 10^3$, and 4×10^3 cm^{-3}, and volume filling factors of $f = 0.1$ and 0.01. These, including turbulence as discussed below, are typical of cold dark clouds (Park & Hong 1995).

We take into account two kinds of internal motions: microturbulence and bulk motion. In the microturbulence models, the cloud is static, and the width of the Gaussian absorption coefficient is attributed to microturbulence which we set to $\sigma_{\rm mic} = 1$ km^{-1} across the cloud. In the cloud models with bulk motion, we assume that the line width is dominated by the random motion of clumps. It is reasonable to assume that the distribution function of the bulk motion is also Gaussian. Even in this case, microturbulence can not be neglected. Thus we set $\sigma_{\rm mic} = 0.2$ km^{-1} and $\sigma_{\rm blk} = 1$ km^{-1}. Overall, the two models have approximately about the same velocity dispersion. The velocity dispersions $\sigma_{\rm mic}$ or $\sigma_{\rm blk}$ mentioned in this work implicitly include a factor of $\sqrt{2}$ relative to the mathematical definition of the standard deviation.

2.2. Molecules

The molecule we are first interested in is CO. CO is, in a sense, an exceptional molecule for RT modeling due to its low dipole moment. It is easily excited to higher levels, and thus, one needs a large number of energy levels. Ten levels and nine transitions in total are taken into account.

We take its frequency, Einstein coefficients, and collisional coefficients from the LAMBDA database (`https://home.strw.leidenuniv.nl/~moldata`). We use the CO-H_2 collision coefficients from Yang et al. (2010) with a ortho-to-para H_2 ratio of 3 as done by Asensio Ramos & Elitzur (2018). Abundance is assumed to be constant across the cloud with 5×10^{-5} relative to molecular hydrogen.

2.3. Proposed Radiative Transfer Code for Clumpy Clouds

Here we describe how the clumpy structure is implicitly implemented into a one-dimensional radiative transfer code. As for the one-dimensional RT model, we adopt and work with the original Monte Carlo code by Bernes (1978).

In order to derive excitation conditions in molecular clouds, one has to solve radiative transfer and statistical equilibrium equations together. The statistical equilibrium equation is solved at given locations in a cloud and needs specific intensity as functions of frequency and angle. The formal solution of radiative transfer for the specific intensity is

$$
\begin{aligned}
I_\nu(r) &= \int_0^{\tau_\nu} S_\nu e^{-\tau'_\nu} d\tau'_\nu + B_\nu e^{-\tau_\nu} \\
&= \int_0^{\tau_\nu} j_\nu e^{-\tau'_\nu} ds + B_\nu e^{-\tau_\nu}.
\end{aligned}
$$

The equation says that the radiation field at a point is given by the background radiation B_ν attenuated by τ_ν and the combination of emission S_ν and attenuation $e^{-\tau_\nu}$ summed over the optical path length τ_ν that depends on direction and frequency. The approach of the Monte Carlo method is different: it separates emission and absorption processes. First it calculates the number of photons generated from the background and those produced spontaneously within the cloud, which correspond to the emission. These real photons are replaced with a smaller, reasonable, number of model photons. The model photons assigned to the background radiation have offset frequencies following a uniform frequency distribution, while the model photons assigned to the internal emission within the cloud follow a Gaussian frequency distribution. The model photons are then allowed to propagate isotropically through the system until they escape the cloud, where only absorption is taken into account. The number of (de-)excitations by the absorption in each zone (spherical shell) is counted and is fed into the rate equation.

We modified the one-dimensional RT code as follows, taking clumpiness into account. We note again that the clumpy structure is *implicitly* realized in the code only via the volume filling factor.

(a) The total number of emitted photons in the cloud is reduced by a factor of f, compared to the completely filled cloud, while that from the background is not affected.

(b) The optical depth of a step length, ds, likewise decreases by a factor f. Intuitively, the optical depth should scale with $f^{1/3}$, since the distance between clumps scales with $f^{-1/3}$. For a proper estimate, consider a small clump of size l immersed in a larger empty volume of size L, where $f = l^3/L^3$. A model cloud is considered a stack of these volumes in x, y, and z directions. The optical depth along a path of length L is $\kappa_\nu l$ if a photon path hits the clump, but zero otherwise. An optical depth averaged over a surface of L^2 perpendicular to the ray direction is then $\kappa_\nu l \times l^2/L^2$ which reduces to $f\kappa_\nu L$. Thus the correction factor is f.

(c) In the original work of Bernes (1979), the number of stimulated absorptions in each zone is counted and divided by the volume of the zone, V_i, where i is the zone index; refer to Equation (5) of Bernes (1979). In the clumpy cloud, the numbers are counted the same way, but must be divided by the actual volume, fV_i, to get the correct transition numbers.

We divided the spherical model cloud into $N_r = 30$ concentric shells of equal thickness in most calculations. The number of model photons is 10^5.

2.4. Verification of Radiative Transfer Code

We test our arguments given above by comparing excitation temperatures derived from the modified 1D calculations with those from 3D computations where the clumpy structure is implemented in a brute force manner. We adopt the 3D model developed by Park & Hong (1995) because it is a simple extension to 3D, keeping all the logic inherent in the 1D Monte Carlo model (Bernes 1979) used in this study. The three-dimensional model divides a spherical volume into $4\pi N^3/3$ small cubics of equal size, while a fraction of cells with non-zero density is considered clumps. In most calculations, we adopted $N = 30$ and 60. The number of model photons is typically 10^6, but for some calculations it is 8×10^6. If the signal-to-noise ration (S/N) is insufficient, we run the code for the same physical parameters three or four times with different seed random numbers, and average the results to get excitation temperatures with reasonable noise levels.

In order to probe the consistency between the 1D and 3D models, we first conducted calculations for a model cloud with $f = 1$, i.e., a filled cloud without bulk motion, and present the resulting excitation temperatures for the lower three transitions of CO in Figure 1. Model parameters for this comparison are $R = 1$ pc, $T_{\rm k} = 15$ K, $n({\rm H_2}) = 1 \times 10^3$, 2×10^3 cm^{-3}, $\sigma_{\rm mic} = 1$ km s^{-1}, $\sigma_{\rm blk} = 0$, and $N_r = N = 30$. Figure 1 indeed shows a good agreement between the two RT models for the conventional cloud model with $f = 1$.

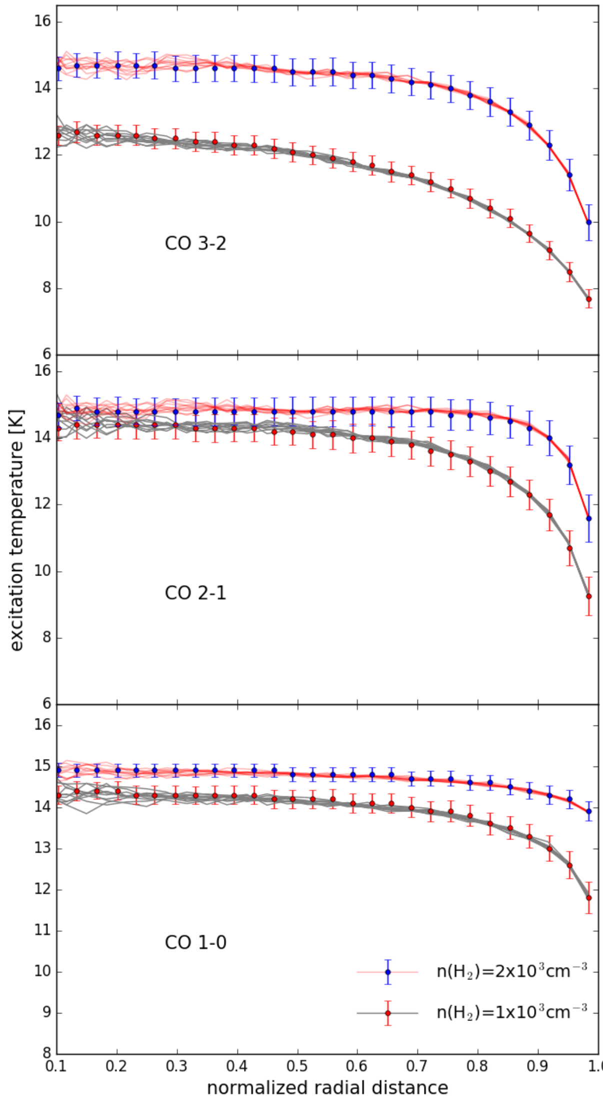

Figure 1. Excitation temperatures of the CO $J = 1-0$, $2-1$, and $3-2$ transitions from 1D and 3D radiative transfer calculations for uniform model clouds with $n({\rm H_2}) = 1 \times 10^3{\rm cm}^{-3}$ and $2 \times 10^3{\rm cm}^{-3}$. For the 1D calculation, the excitation temperatures of the last ten iterations among 50 iterations after settlement are displayed as solid lines, while for the 3D calculations, the mean and standard deviation of excitation temperatures of clumps contained in the concentric shells $[\frac{(n-1)}{N}R, \frac{n}{N}R]$, $(n = 1, 2, ..., N)$ are shown for the last calculation after 40 iterations.

3. Results

3.1. Microturbulent Clouds

We assume that clouds neither have bulk motion nor a systematic motion for this group of model clouds. We set the microturbulence to $\sigma_{\rm mic} = 1$ km s^{-1}. In these models, even clumps separated by a large distance are radiatively coupled. Solid lines in Figure 2 show the excitation temperatures along radial distance for various hydrogen densities and volume filling factors. For comparison, we present excitation temperatures from 3D calculations for $N = 30$ and 60. The results of 3D calculations depend on N or the clump size, particularly for small f. For a fixed f, a larger N indicates a larger number of smaller clumps in the model clouds.

For $f = 0.1$, we find that the results of the one-dimensional calculation are in good agreement with the 3D calculations. The excitation temperatures of the 3D model with the larger N are higher in the deeper part and lower close to the cloud surface, but the difference is very small. The results of the 1D calculation may be considered an extrapolation of the 3D calculations toward the larger N. This is consistent with the interpretation that the 1D calculation implicitly assumes an infinitely large number of small clumps.

In the case of $f = 0.01$, the excitation temperatures are largely uniform. Since there is a significant fraction of empty space, a clump has little chance to interact

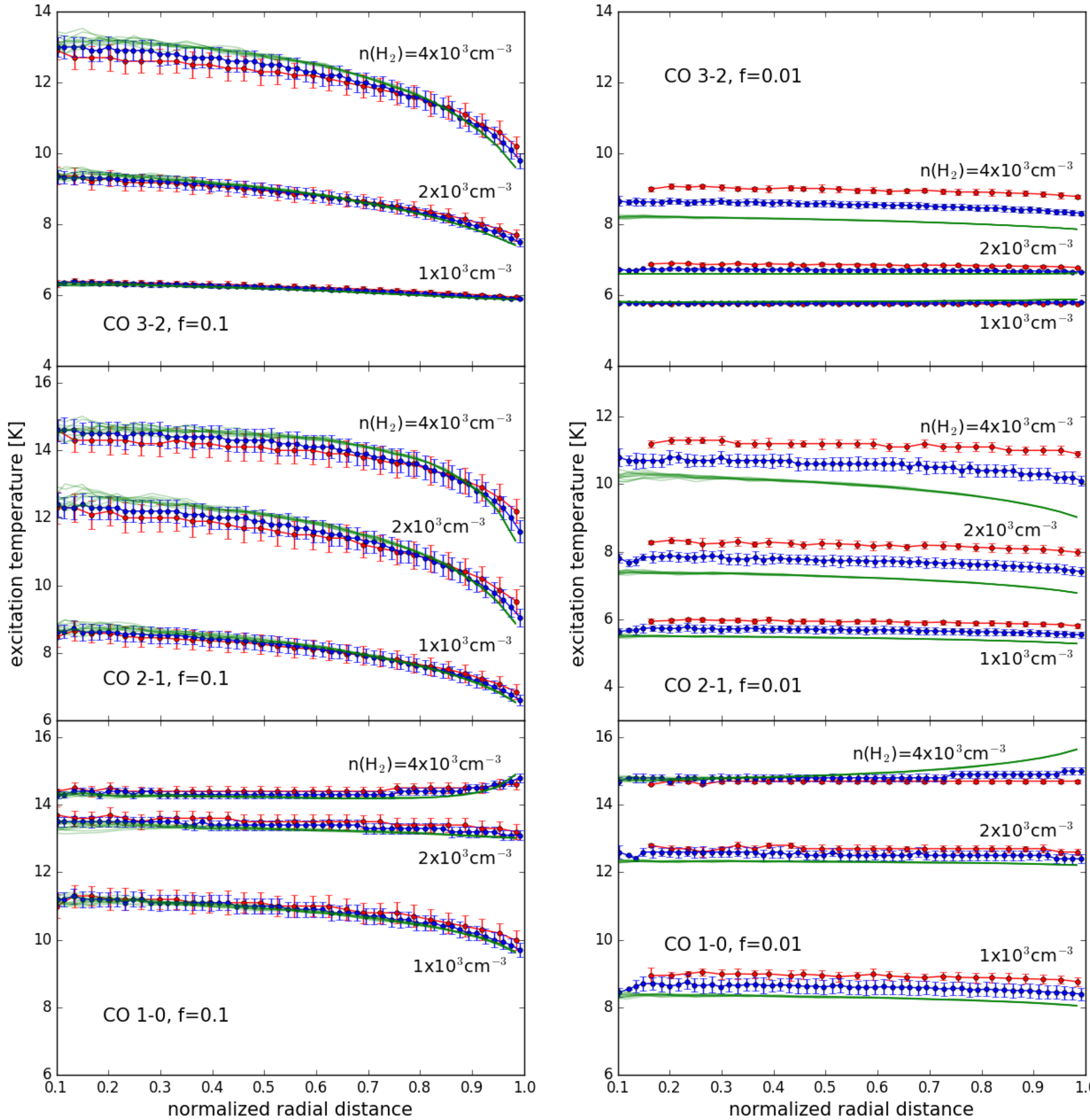

Figure 2. Excitation temperatures of CO $J = 1-0$, $2-1$, and $3-2$ transitions from the proposed 1D and 3D radiative transfer calculations for microturbulent model clouds. Green solid lines are the excitation temperatures of 1D calculations for the last ten iterations among 50 interactions. In the case of 3D calculations, we iterated the code 40 times for $N = 30$ (red lines with error bars) and $N = 60$ (blue lines with error bars). The means and standard deviations are derived as in Figure 1. From the top to bottom of each frame, the density varies from $4 \times 10^3 \mathrm{cm}^{-3}$, $2 \times 10^3 \mathrm{cm}^{-3}$, to $1 \times 10^3 \mathrm{cm}^{-3}$. One can note suprathermal excitation for the model with $4 \times 10^3 \mathrm{cm}^{-3}$.

with clumps in other locations radiatively, but the background radiation can easily penetrate the cloud. The excitation condition of a clump is then determined by its internal radiation and the background radiation, which is reminiscent of the LVG model. Thus the excitation temperatures for small f very weakly depend on the position in the model clouds.

In the figure, for $f = 0.01$ significant differences in excitation temperatures are noted between the 1D and the 3D calculations and between the 3D calculations with $N = 30$ and $N = 60$. Again the excitation conditions of the 1D cloud model are those expected from the extrapolation of 3D calculations. The dependence of the excitation temperatures of the 3D models on the clump size was overlooked in the previous study of Park & Hong (1995). The internal hotter radiation affecting the excitation condition of a clump becomes smaller for smaller clumps; thus the excitation temperatures are lower for smaller clumps. For the $J = 3-2$ transition in the model with $n(\mathrm{H_2}) = 1 \times 10^3$ cm^{-3}, the optical depth of ~ 0.17 through the cloud center is so low that the radiation is dominated by the background

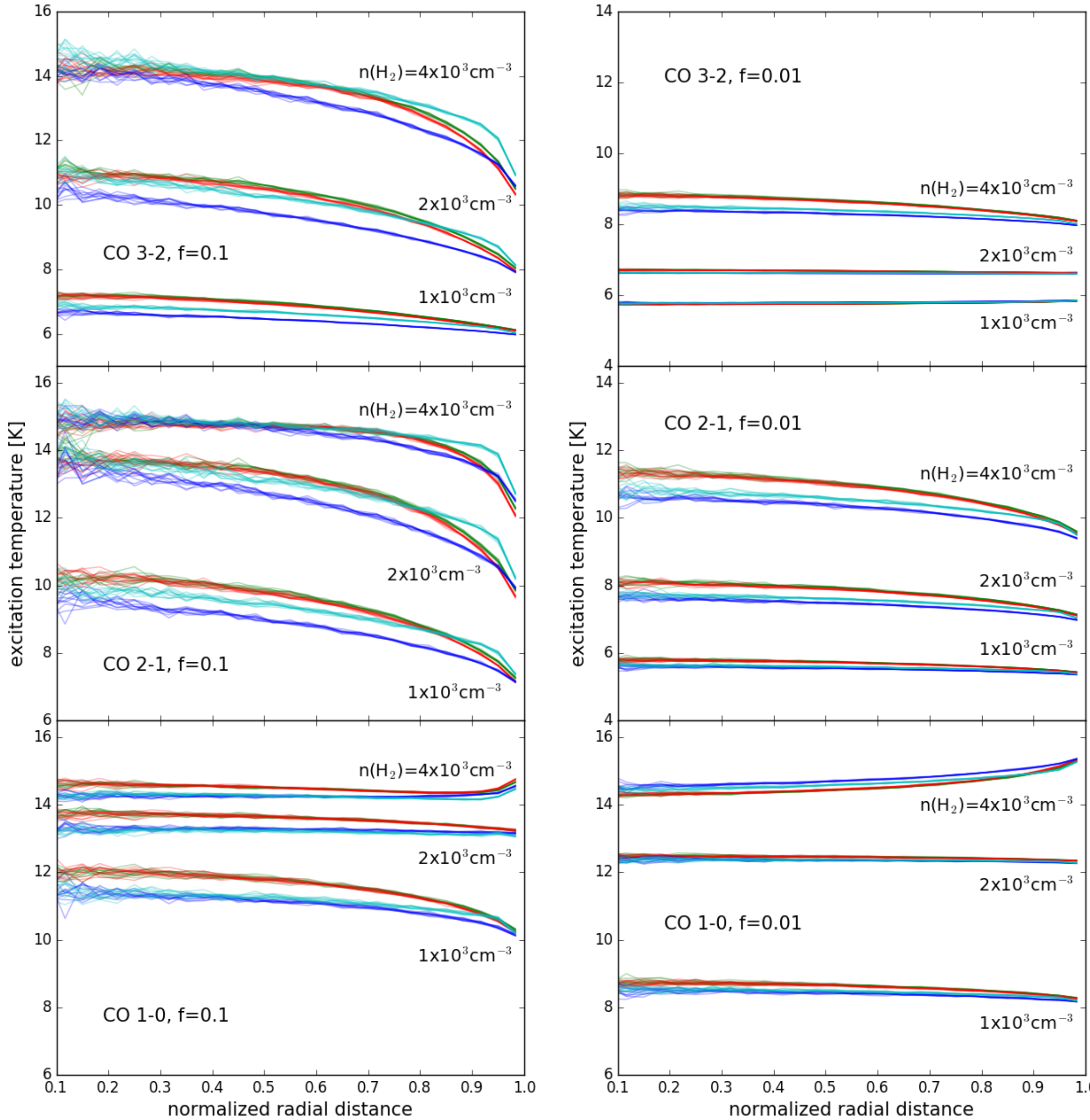

Figure 3. Comparison of the excitation temperatures for two one-dimensional models with bulk motion. Green ($l_{blk} = R/N_r$) and red ($l_{blk} = 0.5R/N_r$) solid lines represent the excitation temperatures for the hybrid models, while blue ($ds = 0.3R/N_r$) and cyan ($ds = 1.2R/N_r$) solid lines indicate the excitation temperatures for the on-the-spot models. Like in Figure 2, the excitation temperatures of the last ten iterations are displayed. From the top to bottom of each frame, the density varies from $4 \times 10^3\mathrm{cm}^{-3}$, $2 \times 10^3\mathrm{cm}^{-3}$, to $1 \times 10^3\mathrm{cm}^{-3}$. See the text for detailed descriptions of the models.

radiation with little contribution from internal radiation. Thus the excitation temperatures converge to a single value, independent of the clump size, as shown in the figure.

In $n(\mathrm{H_2}) = 4 \times 10^3$ cm^{-3} models, the excitation temperature in the outer part is larger than kinetic temperature, suggesting suprathermal excitation. The cloud model of $f = 0.1$ also exhibits the sign of the suprathermal excitation for the same gas density to a lesser degree.

It appears that the modified one-dimensional models for clumpy clouds gives excitation conditions that are consistent with those of 3D calculations.

3.2. Clouds with Bulk Motions

In this model, microturbulence is small and close to thermal motion, i.e., $\sigma_{\mathrm{mic}} = 0.2$ km s^{-1}. Instead, we allow random isotropic bulk motion of clumps with $\sigma_{\mathrm{blk}} = 1$ km s^{-1}. In the 3D model, the bulk motion of clumps is implemented by assigning three-dimensional random motions from Gaussian distributions with $\sigma_{blk,x} = \sigma_{blk,y} = \sigma_{blk,z} = 1/\sqrt{3}$ km s^{-1} to the clumps. This corresponds to one of the many possible states that a cloud model can have. It is not easy to realize this isotropic random motion in the 1D cal-

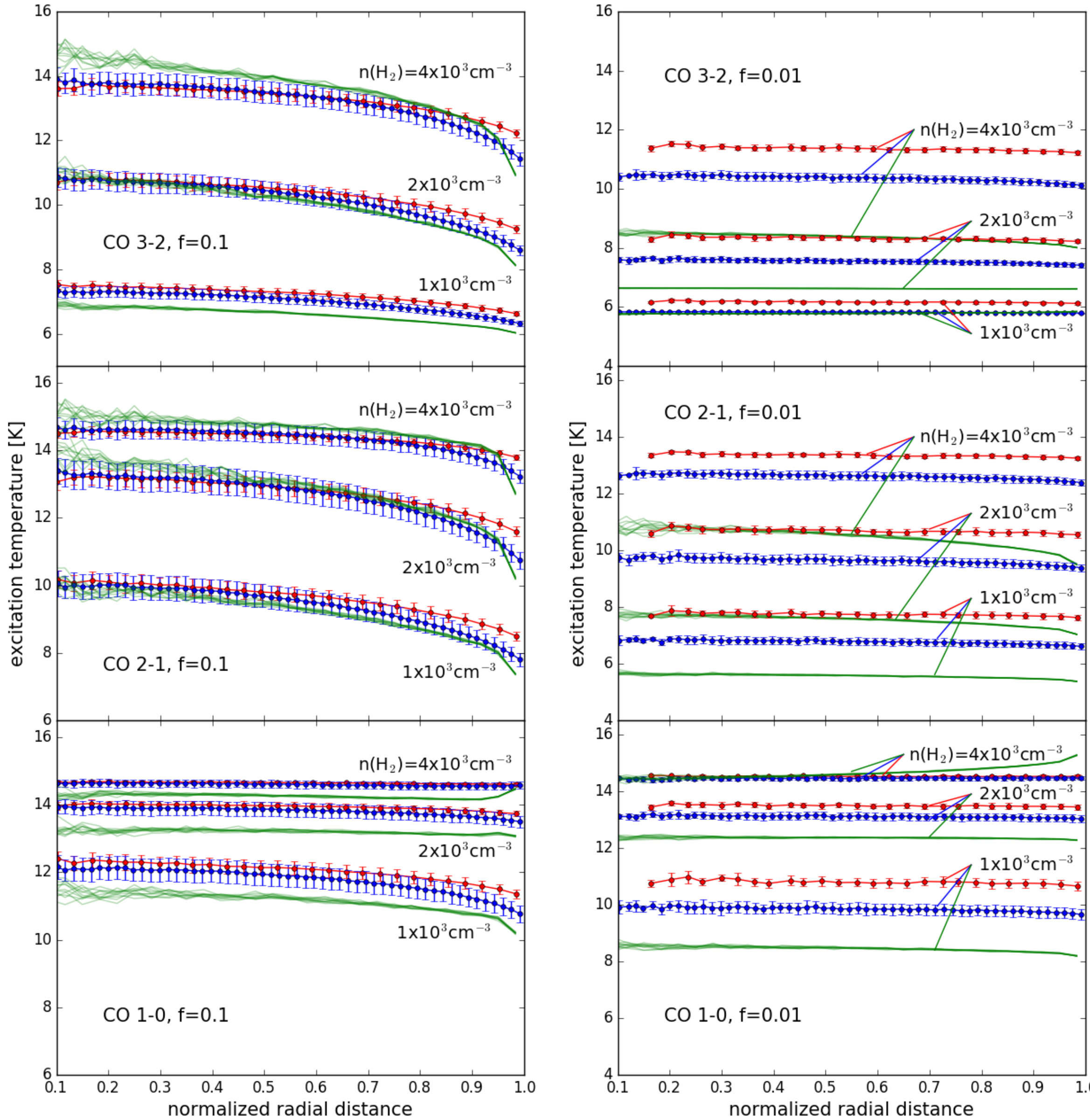

Figure 4. Excitation temperatures of CO $J = 1-0$, $2-1$, and $3-2$ transitions from 1D and 3D radiative transfer calculations for model clouds with bulk motion. Green solid lines are the excitation temperatures of 1D on-the-spot models with $ds = 1.2R/N_r$ for the last ten iterations after settlement. In 3D calculations, we iterated the code 40 times for $N = 30$ (red lines with error bars) and $N = 60$ (blue lines with error bars). From the top to bottom of each frame, the density varies from $4 \times 10^3\mathrm{cm}^{-3}$, $2 \times 10^3\mathrm{cm}^{-3}$, to $1 \times 10^3\mathrm{cm}^{-3}$. One can note suprathermal excitation for the model of $4 \times 10^3\mathrm{cm}^{-3}$ like in Figure 2.

culations. We attack this problem in two ways. The first model may be called a hybrid model, where we devise three-dimensional rectangular grids only for the velocity fields and for tracing photon positions during propagation. After assigning velocity fields to individual grids like in 3D models, we trace photon paths and calculate the line of sight Doppler shift which determines the number of absorption in each zone.

The second approach, that may be called an 'on-the-spot' model, is to assign a one-dimensional random velocity in each propagation step. In this case, we neither need to make a 3D grid for velocity fields nor calculate photon positions in 3D geometry. The velocity along the photon path follows a Gaussian distribution with σ_{blk}. Thus when a clump is passed by different model photons several times, the clump may have different velocities.

In the cloud models with bulk motion, we have a free parameter. For the first model, it is the gridding resolution, l_{blk}; for the second, it is the size of step length ds. They are essentially the same in that they represent a kind of velocity correlation length. In the 3D model, the length may range from the clump size, R/N, to the distance between clumps, $f^{-1/3}R/N$, where N is the number of grids along an axis. But in reality, since there will be numerous small clumps, a much shorter correlation length is expected (Moore & Marscher 1995). Keeping this in mind, we ran the first model for $l_{blk} = (0.5, 1)R/N_r$, while we used $ds = (0.3, 0.6, 1.0, 1.2)R/N_r$ in the second model. Smaller values require a longer calculation time. The resultant excitation temperatures are compared in Figure 3. Calculations show that the excitation temperatures are not sensitive to the l_{blk} for the first model, while they depend on the ds for the second model. Though there are systematic differences, the excitation temperatures are consistent with each other within 1 K. The agreement is better for low optical depth transitions.

In order to compare with 3D models in Figure 4, we adopt the second model with $ds = 1.2R/N_r$ as a representative of models with bulk motion, since it truly reflects the random nature of velocity fields and does not take too much computing time. The excitation temperatures of $f = 0.1$ model clouds exhibit a behavior similar to that of microturbulent model clouds. The 1D and 3D models agree with each other in general, and the excitation conditions of the 1D models roughly correspond to those expected for the 3D models extrapolated to the larger N. The agreement is remarkable considering the differences in computational methods. In the case of $f = 0.01$, the excitation temperatures of the 1D model clouds lie far below those of 3D cloud models. In addition, the excitation conditions of 3D model clouds are more sensitive to the clump size than those of microturbulence models. The size dependence may be understood in terms of the chance of radiative coupling. The probability of radiative interaction is much lower due to the velocity difference among clumps, in addition to the dilution by the small volume filling factor. Therefore, the excitation condition of a clump is far more dependent on the clump size, compared with those of microturbulence models. We again note a sign of suprathermal excitation for the $n(H_2) = 4 \times 10^3$ cm^{-3} models.

Comparing the excitation conditions of 1D calculations of the microturbulence models and the bulk motion models, shown in Figure 2 and Figure 4, we note that the excitation temperatures are closer to each other for $f = 0.01$. The largest difference, less than 1 K, is found for the $J = 2 - 1$ transition of $n(H_2) = 4 \times 10^3$ cm^{-3} models. This is attributed to the fact that if model clouds are optically thin, the bulk motion reduces to microturbulence. The optical depths toward the cloud center of the $n(H_2) = 1 \times 10^3$ cm^{-3} model are found to be 0.41, 0.77, and 0.17 at the line center for $J = 1 - 0$, $2 - 1$, and $3 - 2$ transitions, respectively, while they are 0.71, 2.0, and 1.4 for the model with $n(H_2) = 4 \times 10^3$ cm^{-3}. Thus for the moderate or lower optical depth, $\tau \lesssim 1$, bulk motion is not distinguishable from microturbulence. The proposed model nicely demonstrates the smooth transition of bulk motion from macroturbulence to microturbulence even with the 1D approach. However, we caution that if the model clouds are very optically thin ($\tau \to 0$), then the excitation conditions are independent of the nature of the motion and are determined solely by the background radiation and collisions. The $J = 3 - 2$ transition of the $n(H_2) = 1 \times 10^3$ cm^{-3} cloud corresponds to this case.

4. Discussion and Conclusions

We devised a one-dimensional radiative transfer model that can be applied to clumpy molecular clouds exploiting their stochastic nature, significantly reducing computation time when compared to a 3D model. For microturbulent cloud models, the resulting excitation temperatures are fully consistent with those of three-dimensional calculations. Furthermore, the proposed one-dimensional model gives clues to the excitation conditions that a three-dimensional model cannot provide because a huge number of grids is required. For clouds with bulk motion, the 1D RT model reproduces the excitation conditions reasonably in agreement with those of 3D calculations, though they cannot precisely implement the three-dimensional isotropic velocity field. The bulk motion is found to reduce to microturbulence if the optical depth is moderately thin, demonstrating that the proposed model can integrally deal with the micro- and macro-turbulences. In summary, the new 1D radiative transfer model can be a good proxy for the complicated and time-consuming 3D models, even if it can not completely replace 3D RT models.

3D RT models are more flexible and seem to be closer to reality, but they are slow and require extensive computational resources. 1D RT models have the opposite pros and cons. A simple radiative transfer model, RADEX, adopting the escape probability method, has reached more than 1000 citations as of September 2021 (van der Tak et al. 2007). Therefore there has been an ongoing necessity for simple and handy radiative transfer tools. In this context, the proposed model could be a compromise between the two models. We will test the applicability of the proposed model further, relaxing the condition of uniform density and volume filling factor and taking interclump medium into account.

References

Asensio Ramos, A., & Elitzur, M. 2018, MOLPOP-CEP: An Exact, Fast Code for Multi-level Systems, A&A, 616, A131

Bernes, C. 1978, A Program for Solving Non-LTE, Radiative Transfer Problems with the Monte Carlo Method, Stockholms Obs. Rep. 15

Bernes, C. 1979, A Monte Carlo Approach to Non-LTE Radiative Transfer Problems, A&A, 73, 67

Blitz, L., & Stark, A. A. 1986, Detection of Clump and Interclump Gas in the Rosette Molecule Cloud Complex, ApJL, 300, L89

Brinch, C., & Hogerheijde, M. R. 2010, LIME – A Flexible, Non-LTE Line Excitation and Radiation Transfer Method for Millimeter and Far-infrared Wavelengths, A&A, 523, 25

Goldreich, P., & Kwan, J. 1974, Molecular Clouds, ApJ, 189, 441
Hennebelle, P., & Falgarone, E. 2012, Turbulent Molecular Clouds, A&ARv, 20, 55
Hogerheijde, M. R., & van der Tak, F. F. S. 2000, An Accelerated Monte Carlo Method to Solve Two-dimensional Radiative Transfer and Molecular Excitation. With Applications to Axisymmetric Models of Star Formation, A&A, 362, 697
Juvela, M., 1998 Clumpy Cloud Models for CS and $C^{34}S$ Spectra Observed Towards Southern Massive Star Forming Cores, A&A, 329, 659
Juvela, M., & Padoan, P. 2005, Multiresolution Radiative Transfer for Line Emission, ApJ, 618, 744
Leung, C. M., & Liszt, H. S. 1976, Radiation Transport and Non-LTE Analysis of Interstellar Molecular Lines. I. Carbon Monoxide., ApJ, 208, 732
Molaro, M., Khatri, R., & Sunyaev, R. A. 2016, Probing the Clumping Structure of Giant Molecular Clouds through the Spectrum, Polarisation and Morphology of X-ray Reflection Nebulae, A&A, 589, 88
Moore, E. M., & Marscher, A. P. 1995, Observational Probes of the Small-scale Structure of Molecular Clouds, ApJ, 452, 671
Park, Y.-S., & Hong, S. S. 1995, Excitation and Line Profiles of CO Molecules in Clumpy Interstellar Clouds, A&A, 300, 890
Quenard, D. Bottinelli, S., & Caux, E. 2017, Modelling the 3D Physical Structure of Astrophysical Sources with GASS, MNRAS, 468, 685
Rybarczyk, D. R., Stanimirovic, S., Zweibel, E. G., et al. 2020, Small-scale Structure Traced by Neutral Hydrogen Absorption in the Direction of Multiple-component Radio Continuum Sources, ApJ, 893, 152
van der Tak, F. F. S., Black, J. H., Schoier, F. L., et al. 2007, A Computer Program for Fast Non-LTE Analysis of Interstellar Line Spectra. With Diagnostic Plots to Interpret Observed Line Intensity Ratios, A&A, 468, 627
Yang, B., Stancil, P. C., Balakrishnan, N., & Forrey, R. C. 2010, Rotational Quenching of CO Due to H_2 Collisions, ApJ, 718, 1062